The Astrophysical Journal Supplement Series, 194:22 (6pp), 2011 June doi:10.1088/0067-0049/194/2/22

THE MAGELLANIC QUASARS SURVEY. I. DOUBLING THE NUMBER OF KNOWN ACTIVE GALACTIC NUCLEI BEHIND THE SMALL MAGELLANIC CLOUD

Szymon Kozłowski[1,2], Christopher S. Kochanek[2,3], and Andrzej Udalski[1]
[1] Warsaw University Observatory, Al. Ujazdowskie 4, 00-478 Warszawa, Poland
[2] Department of Astronomy, The Ohio State University, 140 West 18th Avenue, Columbus, OH 43210, USA;
simkoz@astronomy.ohio-state.edu, ckochanek@astronomy.ohio-state.edu
[3] The Center for Cosmology and Astroparticle Physics, The Ohio State University, 191 West Woodruff Avenue, Columbus, OH 43210, USA
Received 2011 February 3; accepted 2011 March 16; published 2011 May 2

ABSTRACT

We report the spectroscopic confirmation of 29 new, 12 plausible, and three previously known quasars behind the central $\sim$1.5 deg^2 region of the Small Magellanic Cloud (SMC). These were identified in a single 2dF/AAOmega observation on the Anglo-Australian Telescope of 268 candidates selected primarily based on their mid-IR colors, along with a smaller number of optically variable sources in OGLE-II close to known X-ray sources. The low detection efficiency was partly expected from the high surface density of SMC as compared with the Large Magellanic Cloud targets and the faintness of many of them (149 with $I > 20$ mag). The expected number of $I < 20$ mag quasars in the field is $\simeq$38, and we found 15 (40%). We did not attempt to determine the nature of the remaining sources, although several appear to be new planetary nebulae. The newly discovered active galactic nuclei can be used as reference points for future proper-motion studies, to study absorption in the SMC interstellar medium, and to study the physics of quasar variability with the existing long-term, highly cadenced OGLE light curves.

Key words: galaxies: active – Magellanic Clouds – quasars: general

Online-only material: color figure, machine-readable table

1. INTRODUCTION

Active galactic nuclei (AGNs) are one of the most important tools in modern cosmology. They are intrinsically the brightest continuously luminous sources in the universe, which allows their detection to great cosmological distances and their use as probes of the universe over cosmic time. AGNs are also believed to play a major role in galaxy evolution (e.g., Heckman et al. 2004), acting as a means for quenching star formation (e.g., Bower et al. 2006; Hickox et al. 2009) and "converting" blue spirals into red elliptical galaxies (e.g., Springel et al. 2005).

Although there are over a hundred thousand known AGNs (e.g., Schneider et al. 2010), it has proved difficult to identify quasars in dense stellar fields such as the Large and Small Magellanic Clouds (LMC and SMC), the Galactic bulge, or other nearby galaxies. For example, the expected number of quasars brighter than OGLE's $I < 20$ mag limit is $\sim$25 deg^{-2} (Figure 13 in Richards et al. 2006), while there are $\sim$150,000 deg^{-2} stars with $I < 20$ mag in the central regions of the SMC. As a result, few quasars are known behind the Magellanic Clouds (57 in the LMC, 28 in the SMC—within a 5° radius),[4] and none have been identified behind the Galactic bulge. Most of the known quasars were found by investigating sources with long timescale, non-periodic variability combined with their colors and magnitudes (e.g., Eyer 2002; Dobrzycki et al. 2003a; Geha et al. 2003; Sumi et al. 2003; Dobrzycki et al. 2005; and recently Kozłowski et al. 2010; MacLeod et al. 2010b; Schmidt et al. 2010; Butler & Bloom 2010; Palanque-Delabrouille et al. 2010; Kim et al. 2011), and a smaller number were found as the (variable) optical counterparts to X-ray sources (Dobrzycki et al. 2002, 2003a, 2003b).

Quasars behind the Magellanic Clouds or the Galactic bulge have several important scientific applications. First, they are the best sources for fixing the reference frames needed for proper-motion studies. The recent improvements in the proper motions of the Magellanic Clouds (Kallivayalil et al. 2006a, 2006b; Piatek et al. 2008) all relied on *Hubble Space Telescope* (*HST*) measurements in fields centered on quasars. The results were surprising, as the Clouds were found to be moving significantly faster than previous estimates (e.g., van der Marel et al. 2002) and the tangential motion of the SMC differs significantly from that of the LMC. This implies that the Clouds may be on their first pericentric passage and unbound from the Galaxy (Besla et al. 2007), and that they may not be bound to each other (Kallivayalil et al. 2006a). These results can be improved not just by longer temporal baselines for the previously known quasars, but also by better mapping out the contaminating internal motions of the Clouds using additional quasar fields. The second familiar reason for finding background quasars is that bright quasars can be used in absorption studies of the SMC interstellar medium (ISM; e.g., Shull et al. 2000; Savage et al. 2000), in particular to probe the gas distribution through the full depth of the SMC. This requires finding the brightest possible quasars behind the Clouds, which is challenging given the density of contaminating sources and the low density of bright quasars, with only $\sim$0.01, 1, and 25 quasars deg^{-2} brighter than $I < 16$, 18, and 20 mag, respectively.

The third application, which may be less familiar, is studying the physics of quasar variability. Kelly et al. (2009) showed that quasar light curves can be well modeled as a damped random walk, a stochastic process with only three parameters: the mean light curve magnitude, a characteristic timescale, and an amplitude. Their study, using $\sim$100 quasars from the

[4] This research has made use of the NASA/IPAC Extragalactic Database (NED) which is operated by the Jet Propulsion Laboratory, California Institute of Technology, under contract with the National Aeronautics and Space Administration.

MACHO survey (Geha et al. 2003) and quasars targeted for reverberation mapping (Giveon et al. 1999; Peterson et al. 2004), found strong correlations between these variability parameters and the physical properties of the quasars such as black hole mass and luminosity. Kozłowski et al. (2010), based on ∼2700 quasar candidates from Kozłowski & Kochanek (2009) with OGLE-III light curves, further demonstrated that the stochastic models describe quasar variability well, using a more powerful statistical approach from Press et al. (1992) and Rybicki & Press (1992, 1994). Recently, MacLeod et al. (2010a) investigated these correlations in greater detail using the light curves of ∼9000 SDSS quasars, finding that the amplitude of variability on long timescales decreases with increasing luminosity and increasing rest-frame wavelength, and that it is also correlated with black hole mass. The characteristic timescale for returning to the mean luminosity increases with increasing wavelength and increasing black hole mass, but remains constant with redshift and luminosity. There are discrepancies, however, between the timescale distributions in MacLeod et al. (2010a) and Kozłowski et al. (2010) which may be due to higher than estimated stellar contamination in Kozłowski et al. (2010), selection differences or the better light curves available for sources in microlensing fields.

The individual parameter estimates for the SDSS quasars are significantly worse than those for the Cloud quasars, and this will also be true of light curves from other modern surveys such as the Catalina Survey (e.g., Larson et al. 2003; Drake et al. 2009), the Palomar Transient Factory (e.g., Law et al. 2009), Pan-STARRS (e.g., Kaiser et al. 2002), or LSST (e.g., LSST Science Collaboration et al. 2009) that attempt to cover large fractions of the sky rather than localized regions. The OGLE microlensing survey has monitored the LMC, SMC, and the Galactic bulge for ∼15 years, providing light curves for 400 million objects (Udalski et al. 1997; Udalski et al. 2008a). These fields have also been observed for shorter periods of time by the EROS (e.g., Tisserand et al. 2007), MACHO (e.g., Alcock et al. 2000), MOA (e.g., Sumi et al. 2005), and SuperMACHO (e.g., Becker et al. 2005) microlensing surveys, aiming primarily at detection of dark matter compact objects in the Galactic halo (e.g., Alcock et al. 2000; Tisserand et al. 2007; Wyrzykowski et al. 2009).

This leaves the problem of identifying the quasars, spectroscopically confirming them, and determining their properties (luminosities, black hole mass estimates from emission line widths). Kozłowski & Kochanek (2009) pointed out that the mid-IR AGN selection method of Stern et al. (2005) would also work reasonably well in dense stellar fields because the mid-IR colors of quasars are different from all normal stars. Based on a simple three-level criterion, they selected ∼5000 quasar candidates behind the Magellanic Clouds from the SAGE (Meixner et al. 2006; Blum et al. 2006) and S3MC (Bolatto et al. 2007) data. In this paper, we present the results of our AAOmega spectroscopic follow-up of a single ∼1.5 deg^2 field in the SMC, containing 268 quasar candidates from Kozłowski & Kochanek (2009). We report the confirmation of 29 new quasars and include a list of 12 plausible quasars. In Section 2 we present the data analysis procedures. In Section 3 we present newly confirmed quasars, and in Section 4 we discuss the detection efficiency. The paper is summarized in Section 5.

2. DATA ANALYSIS

In Kozłowski & Kochanek (2009), we classified the candidates based on three criteria. First, objects in the Stern et al. (2005) mid-IR color selection region were classed as "A" if they lie away from the track of cool blackbodies through the selection region and "B" if they lie close to the track. Second, the brighter sources have mid-IR magnitudes also observed for young stellar objects (YSOs), so sources were classified as "YSO" if they lie in the region heavily contaminated by YSOs and as "QSO" if they did not. Finally, objects with the mid-IR to optical colors typical of quasars were classed as "a," while those which did not were classed as "b." For out first attempt at spectroscopic follow-up, we selected 249 QSO-Aa and 13 QSO-Ba quasar candidates, for a total of 262 targets. The sample included two previously confirmed quasars in the field ($z = 0.563$ and $z = 1.055$; Geha et al. 2003). We also searched for optically variable objects in OGLE-II[5] (Szymański 2005; Udalski et al. 1997) within the 3σ position uncertainties of the X-ray sources from Haberl et al. (2000). We targeted six X-ray/variability-selected objects, including one at $z = 1.06$ confirmed in Dobrzycki et al. (2003a). Since this was an experiment, we did not attempt to exclude known stellar objects from the target list (see Table 2). This was one of several fields prepared for the LMC and SMC, but the only one to be observed.

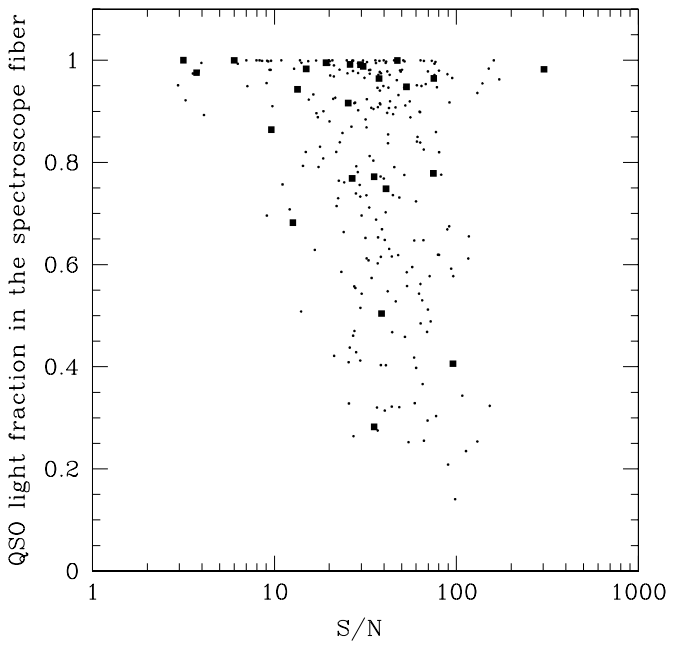

Figure 1. Signal-to-noise ratio (S/N) and stellar flux contamination for each of the 268 observed objects. The stellar flux contaminating a fiber was the contribution from stars within 10 arcsec of each target assuming a 2 arcsec fiber diameter and seeing FWHM. Dots represent all targeted objects, while filled squares are confirmed quasars, and there are no obvious trends in the confirmed fraction with either S/N or contamination.

The field was centered at (R.A., decl.) = (00:52:00.0, −72:48:00.0) J2000. While AAOmega has a field of view of ∼3 deg^2 (Sharp et al. 2006), the S3MC survey had a complex shape so that the actual overlapping area was ∼1.5 deg^2. The spectra were obtained as a service observation on 2009 August 17 in moderate sky conditions with ∼2 arcsec seeing. We used the lowest resolution mode, with $R = 1300$ and a spectral coverage of approximately 5100 Å between the blue (580V) and red (385R) channels. We obtained three exposures of 1800 s, leading to signal-to-noise ratios (S/N) ranging from 3 to 300, with 50% of the objects having S/N > 30 (Figure 1). We used 25 sky fibers, positioned to avoid stellar emission based on the

[5] http://ogledb.astrouw.edu.pl/∼ogle/photdb/

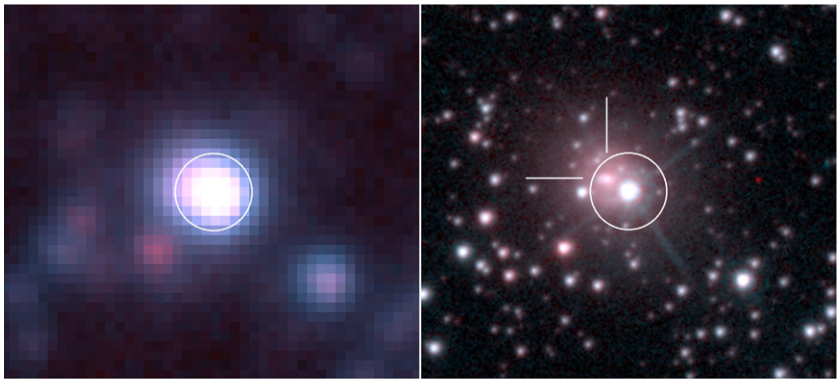

Figure 2. QSO J004818.76−732059.6 at $z = 0.108$, one of our 29 new spectroscopically confirmed quasars, as seen by the OGLE 1.3 m ground-based telescope (left) and *HST* (right). The blue and red colors are for $V/F555W$ and $I/F814W$, respectively. The circle has the 2 arcsec diameter of the AAOmega fibers and is also comparable to the FWHM during the observations. The flux in the fiber is a blended combination of the bright blue star and the fainter, redder extended AGN seen in the *HST* image. The image dimensions are $10'' \times 10''$. North is up and east is to the left.

(A color version of this figure is available in the online journal.)

OGLE-III SMC catalogs (Udalski et al. 2008b). The initial FLD files were created with the Configure software, and the final analysis was done using the 2dfdr software (Taylor et al. 1996).

The most prominent feature of essentially every spectrum is the emission line contribution of the ISM in the SMC. These emission lines are redshifted by ∼2.5 Å, consistent with the radial velocity of the SMC (e.g., Richter et al. 1987). Since the stellar densities are high, contamination from nearby stars is also common, as shown by the OGLE and *HST* images of the "brightest" new AGNs in Figure 2. We estimated the contribution from nearby stars to the flux in the fiber by computing the contribution from stars within 10 arcsec to a 2 arcsec diameter fiber assuming a 2 arcsec FWHM Gaussian seeing profile based on the OGLE-III photometric catalogs (Udalski et al. 2008b). Figure 1 shows our estimate of this contaminating flux from stars relative to the flux of the quasar. Because we are looking for emission line objects, there was no trivial relationship between either S/N or contamination and our ability to identify quasars.

3. NEW QUASARS

We searched each spectrum for the common (redshifted) quasar emission lines (e.g., Vanden Berk et al. 2001) Lyα at 1216 Å, Hδ at 4101 Å, Hγ at 4340 Å, Hβ at 4861 Å, Hα at 6563 Å, magnesium Mg II at 2800 Å, carbon C IV at 1549 Å, and C III] at 1909 Å, as well as the narrow forbidden lines of oxygen [O II] at 3727 Å, [O III] at 4959 Å, or 5007 Å. In general, we required the identification of two lines, except in the redshift range $0.7 < z < 1.2$, where we can only find Mg II despite the broad spectral coverage. We identified 29 new quasars behind the SMC. Their parameters (including the identified lines) are presented in Table 1 (top panel), and their spectra are shown in Figure 3. We also confirmed the three known quasars we included in the target list. Another 12 were plausibly quasars with broad emission lines but remained somewhat ambiguous due to the low quality of their spectra. These objects are listed in Table 1 (middle panel). Table 2 lists the remaining sources and any identifications available from SIMBAD.[6] We have not attempted to classify any of the stellar spectra ourselves.

[6] This research has made use of the SIMBAD database, operated at CDS, Strasbourg, France.

4. DETECTION EFFICIENCY

The low yield requires some discussion. Kozłowski & Kochanek (2009) identified 657 quasar candidates behind the SMC and 4699 behind the LMC. Of these, 215 SMC and 1296 LMC candidates are brighter than $I < 20$ mag corresponding to 72 and 32 candidates per square degree in the SMC and LMC, respectively. The expected number of quasars with $I < 20$ mag is $\sim 25\,\mathrm{deg}^{-2}$ (Richards et al. 2006), so we already had indications that the level of contamination was significantly higher in the SMC/S3MC candidate list than in the LMC/SAGE candidate list. For the roughly 1.5 deg^2 overlap of the S3MC field and the AAOmega field of view, we would expect 38 quasars with $I < 20$ mag. Of the observed 268 quasar candidates we were able to confirm 29 new quasars or 11% of the targets. Of these 29 quasars, 15 are brighter than $I < 20$ mag, which is 40% of the expected number (15 out of an expected 38).

We noted after the observations were complete that there is an ∼0.1 mag blueward shift in the [3.6]–[4.5] colors between the ∼3 deg^2 S3MC data release of Bolatto et al. (2007) used by Kozłowski & Kochanek (2009) and the subsequent release of 30 deg^2 (Gordon & SAGE-SMC Spitzer Legacy Team 2010). This would shift significant numbers of contaminating sources into the mid-IR color selection region. We may also have overestimated the purity of the SMC mid-IR selected sample. This is suggested by the lower density of candidates ($40\,\mathrm{deg}^{-2}$) identified in the LMC by Kim et al. (2011) and that the quasar variability timescale distribution of the mid-IR candidates in Kozłowski et al. (2010) seems to extend to shorter timescales than those in the SDSS sample considered by MacLeod et al. (2010a). We will investigate these issues in more detail once we have completed more spectroscopic fields.

5. SUMMARY

With the identification of 29 quasars, we have doubled the number of known quasars behind the SMC. While the yields were lower than expected, there was already reason to expect this from the difference in the surface density of candidates behind the LMC and SMC in the candidate catalogs of Kozłowski & Kochanek (2009). Fortunately, with the large numbers of fibers available on AAOmega, there is little problem in targeting the candidates. We suspect that the yields in the LMC will be higher.

Identifying large numbers of quasars in the microlensing regions is important not only for use as probes of the LMC/SMC

Table 1
Parameters of 29 New, 12 Plausible, and 3 Previously Known Quasars Behind the SMC.

Name	R.A.	Decl.	V (mag)	I (mag)	z	OGLE-III ID[a]	KK09 Class	Emission Lines	Notes
29 new spectroscopically confirmed quasars									
J003957.65−730603.6	00:39:57.65	−73:06:03.60	19.74	19.44	0.569	125.5.6063	···	H$\delta\gamma$, [O III]	X, V
J004145.04−725435.9	00:41:45.04	−72:54:35.90	20.21	19.05	0.267	126.8.16111	···	[O II], Hβ, [O III]	X, V
J004507.50−724121.8	00:45:07.50	−72:41:21.83	20.10	19.38	2.140	126.3.17176	QSO-Aa	C IV, C III]	···
J004551.62−725735.0	00:45:51.62	−72:57:34.95	20.35	19.34	2.250	126.1.26007	QSO-Ba	C IV, C III]	···
J004736.12−724538.2	00:47:36.12	−72:45:38.19	21.77	20.15	0.572	101.8.38227	QSO-Aa	Mg II, [O II], [O III]	···
J004753.62−724350.6	00:47:53.62	−72:43:50.55	21.21	20.66	2.730	101.8.38968	QSO-Aa	Lyα, C III]	···
J004818.76−732059.6	00:48:18.76	−73:20:59.63	16.57	16.69	0.108	100.8.45221	QSO-Aa	[O II], Hβ, [O III], Hα	Y, X, B1
J004831.50−732339.9	00:48:31.50	−73:23:39.87	21.40	20.32	1.202	100.8.19174	QSO-Aa	C III], Mg II	X
J004944.41−725400.5	00:49:44.41	−72:54:00.53	21.27	20.12	0.569	100.5.55472	QSO-Aa	Mg II, [O III]	···
J005203.27−723830.6	00:52:03.27	−72:38:30.58	20.80	19.90	2.391	101.2.12689	QSO-Aa	Lyα, Si IV, C IV, C III]	···
J005235.03−732940.6	00:52:35.03	−73:29:40.62	19.97	19.66	2.820	103.4.43395	QSO-Aa	Lyα, Si IV, C IV	···
J005254.15−725628.1	00:52:54.15	−72:56:28.07	21.47	20.53	0.288	100.4.26477	QSO-Aa	[O II], [O III]	···
J005259.10−724510.9	00:52:59.10	−72:45:10.93	20.80	20.33	1.930	101.1.53779	QSO-Aa	C IV, C III]	···
J005433.79−730924.0	00:54:33.79	−73:09:23.97	21.61	20.37	1.221	106.5.4994	QSO-Aa	C III], Mg II	···
J005444.70−724813.7	00:54:44.70	−72:48:13.67	21.62	20.73	0.505	105.7.34076	QSO-Aa	[O II], Hβ, [O III]	···
J005613.33−723821.0	00:56:13.33	−72:38:21.00	19.88	18.89	0.489	105.6.41241	QSO-Aa	[O II], Hβ, [O III]	···
J005708.12−722257.8	00:57:08.12	−72:22:57.82	21.49	20.39	0.273	108.8.63047	QSO-Aa	[O II], Hβ, [O III]	···
J005714.13−723342.8	00:57:14.13	−72:33:42.83	20.81	20.05	0.459	105.5.21805	QSO-Aa	[O II], H$\delta\gamma\beta$, [O III]	X
J010005.70−715723.5	01:00:05.70	−71:57:23.53	19.09	18.66	0.882	108.4.10915	QSO-Aa	Mg II, [O II]	X
J010046.02−722131.4	01:00:46.02	−72:21:31.36	20.75	20.05	0.386	108.1.53405	QSO-Aa	[O II], H$\delta\gamma\beta$, [O III]	···
J010057.77−722230.8	01:00:57.77	−72:22:30.82	21.85	20.73	0.465	108.1.55483	QSO-Aa	Mg II, [O II], H$\gamma\beta$, [O III]	X
J010127.75−721306.2	01:01:27.75	−72:13:06.16	20.58	19.79	2.878	113.7.24358	QSO-Aa	Lyα, Si IV, C IV, C III]	X
J010137.52−720418.9	01:01:37.52	−72:04:18.94	19.31	18.51	0.356	113.6.23341	QSO-Aa	[O II], H$\delta\gamma\beta$, [O III]	X, B2
J010151.81−724110.0	01:01:51.81	−72:41:09.95	21.91	20.48	0.302	110.6.2324	QSO-Aa	H$\delta\gamma$, [O III]	···
J010241.90−723238.7	01:02:41.90	−72:32:38.70	19.21	18.91	0.498	110.5.5649	···	H$\delta\gamma\beta$, [O III]	X, V
J010314.92−724307.5	01:03:14.92	−72:43:07.53	19.37	18.45	2.063	110.6.5563	QSO-Aa	C IV, C III]	···
J010315.49−724221.2	01:03:15.49	−72:42:21.19	19.85	19.08	1.777	110.6.5575	QSO-Aa	C IV, C III], Mg II	···
J010425.27−724540.4	01:04:25.27	−72:45:40.42	21.07	20.11	0.130	110.7.29561	QSO-Aa	[O II], Hβ, [O III], Hα	···
J010449.64−724850.5	01:04:49.64	−72:48:50.53	19.69	19.13	2.330	110.7.31965	QSO-Aa	Lyα, C IV	X
12 plausible spectroscopically confirmed quasars									
J004520.77−730301.9	00:45:20.77	−73:03:01.91	21.18	20.52	1.847	125.4.54611	QSO-Aa	C IV, C III], Mg II	···
J004522.89−724541.5	00:45:22.89	−72:45:41.46	21.23	20.77	?	126.2.33358	QSO-Ba	2 broad lines	···
J004542.49−732317.3	00:45:42.49	−73:23:17.27	21.92	20.29	0.785	125.2.55437	QSO-Aa	Mg II, [O II], Hδ	···
J004556.83−725636.5	00:45:56.83	−72:56:36.52	19.24	18.51	1.443	126.1.23941	QSO-Aa	C III], Mg II	···
J004958.75−725952.2	00:49:58.75	−72:59:52.15	20.83	20.12	2.086	100.6.59954	QSO-Aa	C IV, C III]	···
J005132.67−731411.6	00:51:32.67	−73:14:11.57	20.36	19.44	2.450	100.2.11515	QSO-Aa	Lyα, Si IV, C IV, C III]	···
J005454.05−723726.2	00:54:54.05	−72:37:26.17	20.65	19.96	1.780	105.6.35907	QSO-Aa	C III], Mg II	···
J005511.81−723728.3	00:55:11.81	−72:37:28.33	20.59	19.43	0.804	105.6.35056	QSO-Aa	Mg II, [O II], abs. Hδ	···
J005901.04−721330.0	00:59:01.04	−72:13:29.95	20.99	20.47	0.874	108.2.42880	QSO-Aa	Mg II, Hδ?	···
J010005.10−715921.7	01:00:05.10	−71:59:21.65	20.52	19.95	2.716	108.4.11919	QSO-Aa	Lyα, C IV, C III]	X
J010031.06−722444.1	01:00:31.06	−72:24:44.14	19.98	19.07	3.170	108.1.22073	QSO-Aa	Lyα, Si IV, C IV, C III]?	···
J010531.96−723721.3	01:05:31.96	−72:37:21.31	20.25	19.66	1.384	110.6.32667	QSO-Aa	C III], Mg II	···
3 Previously Known Quasars									
J005534.64−722834.4	00:55:34.64	−72:28:34.42	18.70	18.28	0.563	105.5.32347	QSO-Aa	Mg II, H$\delta\gamma\beta$, [O III]	DG
J010128.03−724614.1	01:01:28.03	−72:46:14.11	19.87	19.31	1.055	105.2.38973	QSO-Aa	Mg II	G
J010244.91−721521.9	01:02:44.91	−72:15:21.90	18.90	18.34	1.060	113.7.6604	···	Mg II	X, D

Notes. [a] The OGLE-III ID format is smcXXX.Y.ZZZZZZ, where XXX is the field number, Y is the chip number, and ZZZZZZ is the source number. In the notes column, X is a quasar with the X-ray counterpart (Haberl et al. 2000), B1(B2): sources incorrectly classified as high mass X-ray binaries in Shtykovskiy & Gilfanov (2005) (Haberl & Pietsch 2004), Y: sources incorrectly classified as YSOs in Whitney et al. (2008), and V: sources variable in OGLE-II, D: quasar discovered by Dobrzycki et al. (2003a), and G: quasar discovered by Geha et al. (2003).

through proper motions or absorption studies. It is also important because of the revolution in studying quasar variability that began in 2009 with the introduction of a successful method for quantitatively modeling quasar variability as a damped random walk by Kelly et al. (2009), and its subsequent improvements in Kozłowski et al. (2010) and MacLeod et al. (2010a). With the long, well-cadenced OGLE-II, OGLE-III, and currently OGLE-IV light curves, these new quasars will be invaluable for studying the variability properties of quasars if they can be identified in large enough numbers. Even with the yields of the current observations, we would expect the full Kozłowski & Kochanek (2009) candidate list to produce ∼1000 new quasars.

We thank Rob Sharp, our service time observer, for his help with the AAOmega data reduction. We thank Kris Stanek for helpful comments. We also thank the anonymous referee for helpful suggestions that improved the manuscript. Support for this work was provided by the Polish Ministry of Science and Higher Education through the program "Iuventus Plus," grant number IP2010 020470 to S.K. This work has been

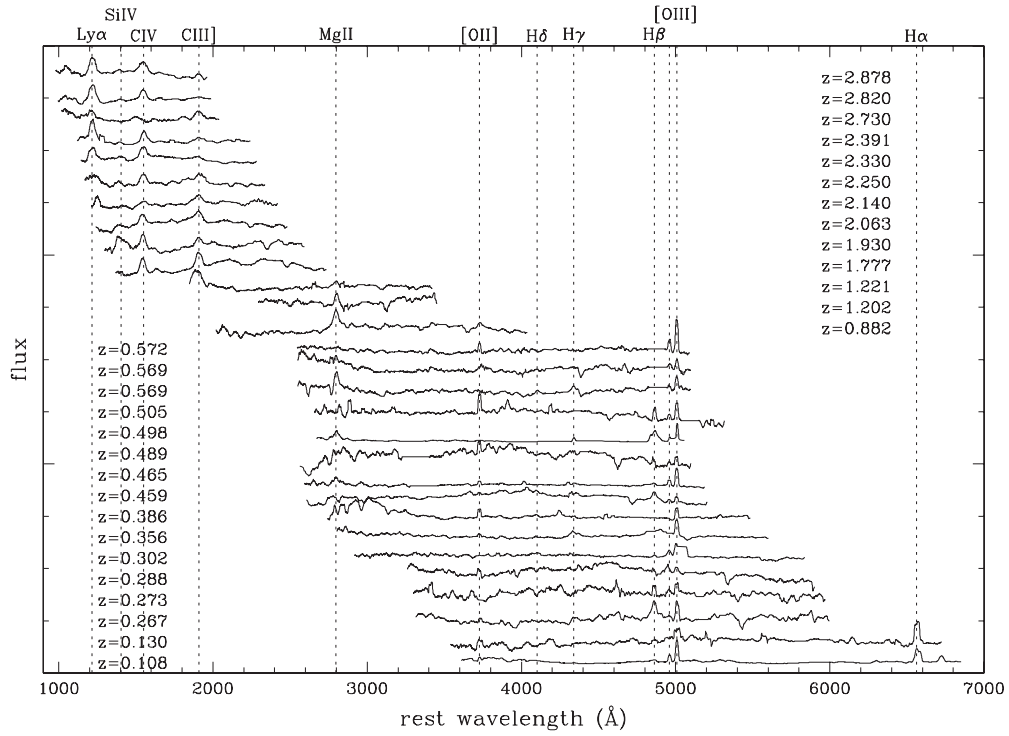

Figure 3. Rest-frame spectra of the 29 new quasars behind the SMC, ordered by redshift. The prominent $z = 0$ contaminating lines found in almost all the spectra have been masked, and we have flattened the continuum in order to focus on the emission lines.

Table 2
Parameters of 224 Remaining Objects With Spectra.

Name	R.A.	Decl.	V (mag)	I (mag)	OGLE-III ID	KK09 Class	Notes
J004413.65−724302.23	00:44:13.65	−72:43:02.23	21.418	20.233	smc126.3.9008	QSO-Aa	Radio
J004520.57−732410.29	00:45:20.57	−73:24:10.29	17.494	19.155	smc125.2.22473	QSO-Aa	PN
J004648.88−732258.26	00:46:48.88	−73:22:58.26	21.235	20.501	smc100.8.4998	QSO-Aa	YSO
J005808.62−720339.19	00:58:08.62	−72:03:39.19	21.394	21.044	smc108.3.31448	QSO-Aa	X-ray
J005820.93−721832.84	00:58:20.93	−72:18:32.84	21.314	20.989	smc108.1.35673	QSO-Aa	EclipsBin
J005732.27−724745.40	00:57:32.27	−72:47:45.40	21.747	20.734	smc105.7.50832	QSO-Ba	–None–

Notes. The column notes includes matches to Simbad objects within 3 arcsec radius, where Radio is a radio source, PN is a planetary nebula, YSO is a young stellar object, X-ray is an X-ray source, EclipsBin is an eclipsing binary and if there is no information on the nature of an object it was marked with "–none–."

(This table is available in its entirety in a machine-readable form in the online journal. A portion is shown here for guidance regarding its form and content.)

supported by NSF grants AST-0708082 and AST-1009756 to C.S.K. and S.K. S.K. and A.U. are also supported by the European Research Council under the European Community's Seventh Framework Programme (FP7/2007–2013), ERC grant agreement no. 246678 to A.U. Based on observations made with the NASA/ESA *Hubble Space Telescope*, obtained from the data archive at the Space Telescope Institute (Program ID 10126, PI: Olszewski). STScI is operated by the association of Universities for Research in Astronomy, Inc. under the NASA contract NAS 5-26555.

REFERENCES

Alcock, C., et al. 2000, ApJ, 542, 281
Becker, A. C., et al. 2005, in IAU Symp. 255, Gravitational Lensing Impact on Cosmology, ed. Y. Mellier & G. Meylan (Cambridge: Cambridge Univ. Press), 357
Besla, G., Kallivayalil, N., Hernquist, L., Robertson, B., Cox, T. J., van der Marel, R. P., & Alcock, C. 2007, ApJ, 668, 949
Blum, R. D., et al. 2006, AJ, 132, 2034
Bolatto, A. D., et al. 2007, ApJ, 655, 212
Bower, R. G., Benson, A. J., Malbon, R., Helly, J. C., Frenk, C. S., Baugh, C. M., Cole, S., & Lacey, C. G. 2006, MNRAS, 370, 645
Butler, N. R., & Bloom, J. S. 2010, AJ, 141, 93
Dobrzycki, A., Eyer, L., Stanek, K. Z., & Macri, L. M. 2005, A&A, 442, 495
Dobrzycki, A., Groot, P. J., Macri, L. M., & Stanek, K. Z. 2002, ApJ, 569, L15
Dobrzycki, A., Macri, L. M., Stanek, K. Z., & Groot, P. J. 2003a, AJ, 125, 1330
Dobrzycki, A., Stanek, K. Z., Macri, L. M., & Groot, P. J. 2003b, AJ, 126, 734
Drake, A. J., et al. 2009, ApJ, 696, 870
Eyer, L. 2002, Acta Astron., 52, 241
Geha, M., et al. 2003, AJ, 125, 1
Giveon, U., Maoz, D., Kaspi, S., Netzer, H., & Smith, P. S. 1999, MNRAS, 306, 637
Gordon, K. D. & SAGE-SMC Spitzer Legacy Team 2010, American Astronomical Society Meeting Abstracts, 215, 459.21
Haberl, F., Filipovic, M. D., Pietsch, W., & Kahabka, P. 2000, A&AS, 142, 41
Haberl, F., & Pietsch, W. 2004, A&A, 414, 667
Heckman, T. M., Kauffmann, G., Brinchmann, J., Charlot, S., Tremonti, C., & White, S. D. M. 2004, ApJ, 613, 109
Hickox, R. C., et al. 2009, ApJ, 696, 891
Kaiser, N., et al. 2002, Proc. SPIE, 4836, 154
Kallivayalil, N., van der Marel, R. P., & Alcock, C. 2006a, ApJ, 652, 1213
Kallivayalil, N., et al. 2006b, ApJ, 638, 772
Kelly, B. C., Bechtold, J., & Siemiginowska, A. 2009, ApJ, 698, 895

Kim, D.-W., Protopapas, P., Byun, Y.-I., Alcock, C., & Khardon, R. 2011, arXiv:1101.3316
Kozłowski, S., & Kochanek, C. S. 2009, ApJ, 701, 508
Kozłowski, S., et al. 2010, ApJ, 708, 927
Larson, S., Beshore, E., Hill, R., Christensen, E., McLean, D., Kolar, S., McNaught, R., & Garradd, G. 2003, BAAS, 35, 982
Law, N. M., et al. 2009, PASP, 121, 1395
LSST Science Collaboration, et al. 2009, LSST Science Book, version 2.0 arXiv:0912.0201
MacLeod, C. L., et al. 2010a, ApJ, 721, 1014
MacLeod, C. L., et al. 2010b, ApJ, 728, 26
Meixner, M., et al. 2006, AJ, 132, 2268
Palanque-Delabrouille, N., et al. 2010, arXiv:1012.2391
Peterson, B. M., et al. 2004, ApJ, 613, 682
Piatek, S., Pryor, C., & Olszewski, E. W. 2008, AJ, 135, 1024
Press, W. H., Rybicki, G. B., & Hewitt, J. N. 1992, ApJ, 385, 404
Richards, G. T., et al. 2006, AJ, 131, 2766
Richter, O.-G., Tammann, G. A., & Huchtmeier, W. K. 1987, A&A, 171, 33
Rybicki, G. B., & Press, W. H. 1992, ApJ, 398, 169
Rybicki, G. B., & Press, W. H. 1994, arXiv:comp-gas/9405004
Savage, B. D., et al. 2000, ApJS, 129, 563
Schmidt, K. B., Marshall, P. J., Rix, H.-W., Jester, S., Hennawi, J. F., & Dobler, G. 2010, ApJ, 714, 1194
Schneider, D. P., et al. 2010, AJ, 139, 2360
Sharp, R., et al. 2006, Proc. SPIE, 6269, 62690G
Shtykovskiy, P., & Gilfanov, M. 2005, MNRAS, 362, 879
Shull, J. M., et al. 2000, ApJ, 538, L73
Springel, V., Di Matteo, T., & Hernquist, L. 2005, ApJ, 620, L79
Stern, D., et al. 2005, ApJ, 631, 163
Sumi, T., et al. 2003, ApJ, 591, 204
Sumi, T., et al. 2005, MNRAS, 356, 331
Szymański, M. K. 2005, Acta Astron., 55, 43
Taylor, K., Bailey, J., Wilkins, T., Shortridge, K., & Glazebrook, K. 1996, in ASP Conf. Ser. 101, Astronomical Data Analysis Software and Systems V, ed. G. H. Jacoby & J. Barnes (San Francisco, CA: ASP), 195
Tisserand, P., et al. 2007, A&A, 469, 387
Udalski, A., Kubiak, M., & Szymański, M. K. 1997, Acta Astron., 47, 319
Udalski, A., Szymański, M. K., Soszyński, I., & Poleski, R. 2008a, Acta Astron., 58, 69
Udalski, A., et al. 2008b, Acta Astron., 58, 329
Vanden Berk, D. E., et al. 2001, AJ, 122, 549
van der Marel, R. P., Alves, D. R., Hardy, E., & Suntzeff, N. B. 2002, AJ, 124, 2639
Whitney, B. A., et al. 2008, AJ, 136, 18
Wyrzykowski, Ł., et al. 2009, MNRAS, 397, 1228